IERCU

Institute of Economic Research, Chuo University

Discussion Paper No.203

Learning in Monopolies with Delayed Price Information

Akio Matsumoto
Chuo University

Ferenc Szidarovszky
University of Pécs

April 2013

IERCU Discussion Paper

INSTITUTE OF ECONOMIC RESEARCH
Chuo University
Tokyo, Japan

Learning in Monopolies with Delayed Price Information*

Akio Matsumoto† Chuo University

Ferenc Szidarovszky‡ University of Pécs

Abstract

We call the intercept of the price function with the vertical axis the *maximum price* and the slope of the price function the *marginal price*. In this paper it is assumed that a monopoly has full information about the marginal price and its own cost function but is uncertain on the maximum price. However, by repeated interaction with the market, the obtained price observations give a basis for an adaptive learning process. It is also assumed that the price observations have fixed delays, so the learning process can be described by a delayed differential equation. In the cases of one or two delays, the asymptotic behavior of the resulting dynamic process is examined, stability conditions are derived and the occurrence of Hopf bifurcation is shown at the critical values. It is also shown that the nonlinear learning process can generate complex dynamics when the steady state is locally unstable and the delay is long enough.

Keywords: Bounded rationallity, Monopoly dynamics, Fixed time delay, Adaptive learning, Hopf bifurcation

JEL Classification : C62, C63, D21, D42

*The authors highly appreciate the financial supports from the Japan Society for the Promotion of Science (Grant-in-Aid for Scientific Research (C) 24530202) and Chuo University Grant for Special Research and Joint Research Grant 0981).

†Professor, Department of Economics, Chuo University, 742-1, Higashi-Nakano, Hachioji, Tokyo, 192-0393, Japan; akiom@tamacc.chuo-u.ac.jp

‡Professor, Department of Applied Mathematics, Universeity of Pécs, Ifjúság, u 6, H-7624, Pécs, Hungary; szidarka@gmail.com

1 Introduction

This paper uses the familiar monopoly model in which there is only one firm having linear price and cost functions. Its main purpose is to show how cyclic and erratic dynamics can emerge from quite simple economic structures when uncertainty, information delays and behavioral nonlinearites are present. Implicit in the text-book approach is an assumption of complete and instantaneous information availability on price and cost functions. In consequence, the monopoly can choose its optimal choices of price and quantity to maximize profit. Moreover the monopoly model becomes static in nature. The assumption of such a rational monopoly is, however, questionable and unrealistic in real economies, since there are always uncertainty and a time delay in collecting information and determining optimal responses, and in addition, function relations such as the market price function cannot be determined exactly based on theoretical consideration and observed data. Getting closer to the real world and improving the monopoly theory, we replace this extreme but convenient assumption with the more plausible one. Indeed, the firm is assumed, first, to have only limited knowledge on the price function and, second, to obtain it with time delay. As a natural consequence of these alternations, the firm gropes for its optimal choice by using data obtained through market experiences. The modified monopoly model becomes dynamic in nature.

In the literature, there are two different ways to model time delays in continuous-time scale: fixed time delay and continuously distributed time delay (fixed delay and continuous delay henceforth). The former is applicable when an institutionally or socially determined fixed period of time delay is presented for the agents involved. The latter is appropriate for economic situations in which different lengths of delays are distributed over heterogeneous agents or the length of the delay is random depending on unforeseeable circumstance. The choice of the type of delay has situation-dependency and results in the use of different analytical tools. In the cases of fixed delay, dynamics is described by a delay differential equation whose characteristic equation is a mixed polynomial-exponential equation with infinitely many eigenvalues. Burger (1956), Bellman and Cooke (1956) and Cooke and Grossman (1992) offer methodology of complete stability analysis in such models. Fixed delay dynamics has been investigated in various economic frameworks including microeconomics (i.e., oligopoly dynamics) and macroeconomics (i.e., business cycle). On the other hand, in the cases of continuous delay, Volterra-type integro-differential equations are used to model the dynamics. The theory of continuous delays with applications in population dynamics is offered by Cushing (1977). Since Invernizzi and Medio (1991) have introduced continuous delays into mathematical economics, its methodology is used in analyzing many economic dynamic models.

This paper continues monopoly dynamics considered by Matsumoto and Szidarovszky (2012d) where the monopoly does not know the price function and fixed time delays are introduced into the output adjustment process based on

the gradient of the expected profit.[1] It also aims to complement Matsumoto and Szidarovszky (2012a,b) where uncertain delays are modeled by continuous delays when the firm wants to react to average past information instead of sudden market changes. Gradient dynamics is replaced with an adaptive learning scheme based on profit maximizing behavior. Although there is price uncertainty and the price information is delayed, the monopoly is still able to update its estimate on the price function via the usage of price observations and its optimal price beliefs. We will consider the cases of a single delay and two delays, respectively, and then demonstrate a variety of dynamics ranging from simple cyclic oscillations to complex behavior involving chaos.

This paper develops as follows. After the mathematical model is formulated, the case of a single delay is examined, when the firm uses the most current delayed price information to form its expectation about the maximum price. Then it is assumed that the firm formulates its price expectation based on two delayed observations by using a linear prediction scheme. We will consider three cases here with slightly different asymptotic behavior. In all cases complete stability analysis is given, the stability regions are determined and illustrated. The occurrence of Hopf bifurcation is shown at the critical values of the bifurcation parameter, which is the length of the single delay or one of the two delays. The last section offers conclusions and further research directions.

2 The Mathematical Models

Consider a single product monopoly that sells its product to a homogeneous market. Let q denote the output of the firm, $p(q) = a - bq$ the price function and $C(q) = cq$ the cost function.[2] Since $p(0) = a$ and $|\partial p(q)/\partial q| = b$, we call a the *maximum price* and b the *marginal price*. There are many ways to introduce uncertainty into this framework. In this study, it is assumed that the firm knows the marginal price but does not know the maximum price. In consequence it has only an estimate of it at each time period, which is denoted by $a^e(t)$. So the firm believes that its profit is

$$\pi^e = (a^e - bq)q - cq$$

and its best response is

$$q^e = \frac{a^e - c}{2b}.$$

[1] In the framework with discrete-time scale, Puu (1995) shows that the boundedly rational monopoly behaves in an erratic way under cubic demand function and production delay. Naimzada and Ricchiuti (2008) also show that complex dynamics can arise in a nonlinear and delay monopoly with a rule of thumb. Naimzada (2012) exhibits that delay monopolistic dynamics can be described by the well-known logistic equation when the firm takes a sspecial learning scheme. More recently Matsumoto and Szidarovszky (2013) consider dynamics of a boundedly rational monopoly and show that the monopoly equilibrium undergoes to complex dynamics through either a period-doubling or a Neimark-Sacker bifurcation.

[2] Linear functions are assumed only for the sake of simplicity. We can obtain a similar learning process to be defined even if both functions are nonlinear. It is also assumed for the sake of simplicity that the firm has perfect knowledge of production technology (i.e., cost function).

Further, the firm expects the market price to be

$$p^e = a^e - bq^e = \frac{a^e + c}{2}. \tag{1}$$

However, the actual market price is determined by the real price function

$$p^a = a - bq^e = \frac{2a - a^e + c}{2}. \tag{2}$$

Using these price data, the firm updates its estimate. The simplest way for adjusting the estimate is the following. If the actual price is higher than the expected price, then the firm shifts its believed price function by increasing the value of a^e, and if the actual price is the smaller, then the firm decreases the value of a^e. If the two prices are the same, then the firm wants to keep its estimate of the maximum price. This adjustment or learning process can be modeled by the differential equation

$$\dot{a}^e(t) = k\left[p^a(t) - p^e(t)\right],$$

where $k > 0$ is the speed of adjustment. Substituting relations (1) and (2) reduces the adjustment equation to a linear differential equation with respect to a^e as

$$\dot{a}^e(t) = k\left[a - a^e(t)\right]. \tag{3}$$

In another possible learning process, the firm revises the estimate in such a way that the growth rate of the estimate is proportional to the difference between the expected and actual prices. Replacing $\dot{a}^e(t)$ in equation (3) with $\dot{a}^e(t)/a^e(t)$ yields a different form of the adjustment process

$$\frac{\dot{a}^e(t)}{a^e(t)} = k\left[a - a^e(t)\right]$$

or multiplying both sides by $a^e(t)$ generates the logistic model

$$\dot{a}^e(t) = ka^e(t)\left[a - a^e(t)\right] \tag{4}$$

which is a nonlinear differential equation.

If there is a time delay τ in the estimated price, then we can rewrite the estimated price and market price at time t based on information at time $t - \tau$ as

$$p^e(t; t-\tau) = a^e(t-\tau) - bq^e(t; t-\tau)$$

and

$$p^a(t; t-\tau) = a - bq^e(t; t-\tau)$$

where $q^e(t; t-\tau)$ is the delay best reply,

$$q^e(t; t-\tau) = \frac{a^e(t-\tau) - c}{2b}.$$

Then equations (3) and (4) have to be modified, respectively, as

$$\dot{a}^e(t) = k\left[a - a^e(t-\tau)\right] \tag{5}$$

and

$$\dot{a}^e(t) = ka^e(t)\left[a - a^e(t-\tau)\right]. \tag{6}$$

If the firm uses two past price information, then the delay dynamic equations turn to be

$$\dot{a}^e(t) = k\left[a - \omega a^e(t-\tau_1) - (1-\omega)a^e(t-\tau_2)\right] \tag{7}$$

and

$$\dot{a}^e(t) = ka^e(t)\left[a - \omega a^e(t-\tau_1) - (1-\omega)a^e(t-\tau_2)\right] \tag{8}$$

where τ_1 and τ_2 denote the delays in the price information. If the firm uses interpolation between the observations, then $0 < \omega < 1$, and if it uses extrapolation to predict the current price, then the value of ω can be negative or even greater than unity. Notice that for $\omega = 0$ and $\omega = 1$, equations (7) and (8) reduce to equations (5) and (6). If $0 < \omega < 1$, then the cases of $\omega \leq 1/2$ are the same as $\omega \geq 1/2$ because of the symmetry of the model between τ_1 and τ_2. Similarly, if $\omega < 0$, then $1 - \omega > 1$, so the cases of $\omega < 0$ and $\omega > 1$ are also equivalent. Therefore in models (7) and (8), we will assume that $\omega \geq 1/2$ and $\omega \neq 1$.

By introducing the new variable $z(t) = a^e(t) - a$, equation (5) and the linearized version of equation (6) are written as

$$\dot{z}(t) + \alpha z(t-\tau) = 0 \tag{9}$$

where $\alpha = k$ or $\alpha = ak$. By the same way, equation (7) and the linearized version of equation (8) are modified as

$$\dot{z}(t) + \alpha\omega z(t-\tau_1) + \alpha(1-\omega)z(t-\tau_2) = 0. \tag{10}$$

In the following sections, we will examine the asymptotic behavior of the trajectories of equations (9) and (10).

3 Single Fixed Delay

If there is no delay, then $\tau = 0$ and equation (9) becomes an ordinary differential equation with characteristic polynomial $\lambda + \alpha$. So the only eigenvalue is negative implying the global asymptotic stability of the steady state $\bar{z} = 0$ if the original equation is linear and the local asymptotic stability if nonlinear. The steady state corresponds to the true value of the maximum price. If $\tau > 0$, then the exponential form $z(t) = e^{\lambda t}u$ of the solution gives the characteristic equation,

$$\lambda + \alpha e^{-\lambda\tau} = 0. \tag{11}$$

Since the only eigenvalue is negative at $\tau = 0$, we expect asymptotical stability for sufficiently small values of τ and loss of stability for sufficiently large values

of τ. If the steady state becomes unstable, then stability switch must occur when $\lambda = i\nu$. If λ is an eigenvalue, then its complex conjugate is also an eigenvalue. In consequence we can assume, without any loss of generality, that $\nu > 0$. So equation (11) can be written as

$$i\nu + \alpha e^{-i\nu\tau} = 0.$$

By separating the real and imaginary parts, we have

$$\alpha \cos \nu\tau = 0$$

and

$$\nu - \alpha \sin \nu\tau = 0.$$

Therefore

$$\cos \nu\tau = 0 \text{ and } \sin \nu\tau = \frac{\nu}{\alpha}$$

with $\nu = \alpha$ leading to infinitely many solutions,

$$\tau = \frac{1}{\alpha}\left(\frac{\pi}{2} + 2n\pi\right) \text{ for } n = 0, 1, 2, ... \tag{12}$$

The solution τ with $n = 0$ forms a downward-sloping curve with respect to α,

$$\tau^* = \frac{\pi}{2\alpha} \text{ with } \alpha = k \text{ or } \alpha = ak.$$

Applying the main theorem in Hayes (1950) or the same result obtained differently in Szidarovszky and Matsumoto (2012c), we can find that this curve divides the non-negative (α, τ) plane into two subregions; the real parts of the roots of the characteristic equation are all negative in the region below the curve and some roots are positive in the region above. This curve is often called a *partition curve* separating the stability region from the instability region. Notice that the critical value of τ decreases with α, so a larger value of α caused by the high speed of adjustment and/or the larger maximum price makes the steady state less stable.

We can easily prove that all pure complex roots of equation (11) are single. If λ is a multiple eigenvalue, then

$$\lambda + \alpha e^{-\lambda\tau} = 0$$

and

$$1 + \alpha e^{-\lambda\tau}(-\tau) = 0$$

implying that

$$1 + \lambda\tau = 0$$

or

$$\lambda = -\frac{1}{\tau}$$

which is a real and negative value.

In order to detect stability switches and the emergence of a Hopf bifurcation, we select τ as the bifurcation parameter and consider λ as function of τ, $\lambda = \lambda(\tau)$. By implicitly differentiating equation (11) with respect to τ, we have

$$\frac{d\lambda}{d\tau} + \alpha e^{-\lambda\tau}\left(-\frac{d\lambda}{d\tau}\tau - \lambda\right) = 0$$

implying that

$$\frac{d\lambda}{d\tau} = -\frac{\lambda^2}{1+\tau\lambda}$$

and as $\lambda = i\nu$, its real part becomes

$$\begin{aligned}\mathrm{Re}\left(\frac{d\lambda}{d\tau}\right) &= \mathrm{Re}\left(\frac{\nu^2}{1+i\tau\nu}\right) \\ &= \frac{\nu^2}{1+(\tau\nu)^2} > 0.\end{aligned}$$

At the critical value of τ, the sign of the real part of an eigenvalue changes from negative to positive and it is a Hopf bifurcation point of the nonlinear learning process (6) with one delay that has a family of periodic solutions. Thus we have the following results.

Theorem 1 *(1) For the linear adjustment process (5), stability of the steady state is lost at the critical value of* τ,

$$\tau^* = \frac{\pi}{2k}$$

and cannot be regained for larger values of $\tau > \tau^*$. *(2) For the logistic adjustment process (6), stability of the steady state is lost at*

$$\tau^{**} = \frac{\pi}{2ak}$$

and limit cycles appear through Hopf bifurcation for $\tau > \tau^{**}$.

An intuitive reason why stability switch occurs only at the critical value of τ with $n = 0$ is the following. Notice first that the delay differential equation has infinitely many eigenvalues and second that their real parts are all negative for $\tau < \tau^*$. When increasing τ arrives at the partition curve, then the real part of one eigenvalue becomes zero and its derivative with respect to τ is positive implying that the real part changes its sign to positive from negative. Hence the steady state loses stability at this critical value. Further increasing τ crosses the (α, τ) curve defined by equation (12) with $n = 1$. There the real part of another eigenvalue changes its sign to positive from negative. Repeating the same arguments, we see that stability cannot be regained and therefore no stability switch occurs for any $n \geq 1$. Hence stability is changed only when τ crosses the partition curve.

Theorem 1 is numerically confirmed. In Figure 1(A), three cyclic trajectories generated by the linear delay equation (5) are depicted under $a = 1$ and $k = 1$. The initial functions are the same, $\phi(t) = 0.5$ for $t \leq 0$ but lengths of delay are different. The blue trajectory with $\tau = \tau^* - 0.1$ shows damped oscillation approaching the steady state, the black trajectory with $\tau = \tau^*$ converges to a limit cycle (i.e., a degenerated Hopf cycle) and the red trajectory with $\tau = \tau^* + 0.1$ cyclically diverges away from the steady state. On the other hand, in Figure 1(B), one limit cycle generated by the logistic delay equation (6) is illustrated under the same parametric conditions, the same initial function and $\tau = \tau^{**} + 0.05$. By comparing these numerical results, it is quite evident that nonlinearity of the logistic equation can be a source of persistent fluctuations when the steady state loses its stability.

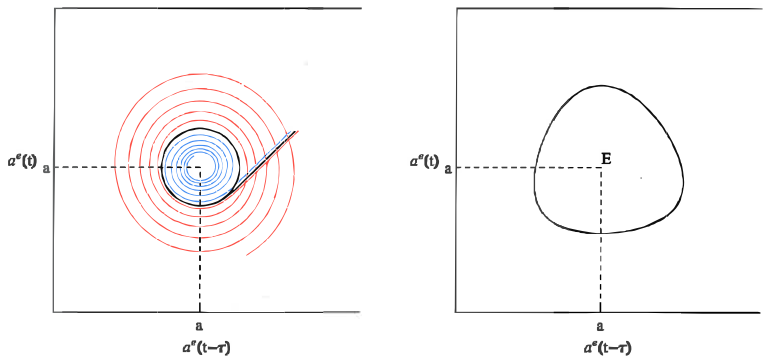

(A) Linear learning (B) Nonlinear learning

Figure 1. Cyclic fluctuations

4 Two Fixed Delays

In this section, we draw attention to asymptotic behavior of differential equation (8) with two delays. Its characteristic equation is obtained by substituting the exponential form $q(t) = e^{\lambda t}u$ into equation (10) and arranging the terms:

$$\lambda + \alpha\omega e^{-\lambda\tau_1} + \alpha(1-\omega)e^{-\lambda\tau_2} = 0$$

or

$$\bar{\lambda} + \omega e^{-\bar{\lambda}\gamma_1} + (1-\omega)e^{-\bar{\lambda}\gamma_2} = 0 \tag{13}$$

where $\bar{\lambda} = \lambda/\alpha$, $\gamma_1 = \alpha\tau_1$ and $\gamma_2 = \alpha\tau_2$. If $\gamma_1 = \gamma_2 = 0$ (or $\tau_1 = \tau_2 = 0$), then the steady state is asymptotically stable, since the only eigenvalue is negative. In order to find stability switches, we assume again that $\bar{\lambda} = i\nu$ with $\nu > 0$. Then equation (13) becomes

$$i\nu + \omega e^{-i\nu\gamma_1} + (1-\omega)e^{-i\nu\gamma_2} = 0.$$

Separating the real and imaginary parts yields

$$\omega \cos \nu\gamma_1 + (1-\omega)\cos \nu\gamma_2 = 0 \tag{14}$$

and

$$\nu - \omega \sin \nu\gamma_1 - (1-\omega)\sin \nu\gamma_2 = 0 \tag{15}$$

when $\omega \geq 1/2$ and $\omega \neq 1$ are assumed. We first examine two boundary cases, one with $\gamma_1 = 0$ and the other with $\gamma_2 = 0$, to obtain the following two results.

Theorem 2 *If $\gamma_1 = 0$, then the steady state is locally asymptotically stable for all $\gamma_2 > 0$.*

Proof. In the case of $\gamma_1 = 0$, equation (14) is reduced as

$$\cos \nu\gamma_2 = -\frac{\omega}{1-\omega}.$$

If $\omega = 1/2$, then $\cos \nu\gamma_2 = -1$ so $\sin \nu\gamma_2 = 0$ implying that $\nu = 0$, which is a contradiction. If $1/2 < \omega < 1$, then $-\omega/(1-\omega) < -1$, so no solution exists. If $\omega > 1$, then $-\omega/(1-\omega) > 1$, so there is no solution either. Therefore equation (13) has no pure imaginary roots that cross the imaginary axis when γ_2 increases from zero. ■

Putting this result differently, we can say that for $\gamma_1 = 0$, delay γ_2 is *harmless* implying that the steady state is locally asymptotically stable regardless of the values of γ_2. We now proceed to the other case.

Theorem 3 *If $\gamma_2 = 0$ and $\omega > 1/2$, then the steady state is locally asymptotically stable for $0 < \gamma_1 < \gamma_1^*$ and locally unstable if $\gamma_1 > \gamma_1^*$ where the critical value of γ_1 is defined as*

$$\gamma_1^* = \frac{\cos^{-1}\left(-\frac{1-\omega}{\omega}\right)}{\sqrt{2\omega - 1}}.$$

Proof. In the case of $\gamma_2 = 0$, (14) and (15) are reduced to

$$(1-\omega) + \omega \cos \nu\gamma_1 = 0$$

and

$$\nu - \omega \sin \nu\gamma_1 = 0.$$

Moving $1-\omega$ and ν to the right hand sides, squaring both sides and adding the resulted equations yield

$$\nu^2 = 2\omega - 1.$$

The positive solution of ν is

$$\nu = \sqrt{2\omega - 1}$$

where $\omega > 1/2$. Substituting this value into the first equation above and solving the resultant equation, we have γ_1^*, the critical value of γ_1. In the same way

as in proving Theorem 1, we arrive at the stability result by applying Hays' theorem or our result in Szidarovszky and Matsumoto (2012c). ■

We now examine the general case of $\gamma_1 > 0$ and $\gamma_2 > 0$. By introducing the new variables

$$x = \sin \nu\gamma_1 \text{ and } y = \sin \nu\gamma_2,$$

equation (14) implies that

$$\omega^2(1-x^2) = (1-\omega)^2(1-y^2)$$

or

$$-\omega^2 x^2 + (1-\omega)^2 y^2 = 1 - 2\omega \tag{16}$$

and from (15),

$$y = \frac{\nu - \omega x}{1-\omega}. \tag{17}$$

By combining (16) and (17), we get an equation for x,

$$-\omega^2 x^2 + (1-\omega)^2 \left(\frac{\nu - \omega x}{1-\omega}\right)^2 = 1 - 2\omega$$

implying that

$$x = \frac{\nu^2 + 2\omega - 1}{2\nu\omega}$$

and from (17),

$$y = \frac{\nu^2 - 2\omega + 1}{2\nu(1-\omega)}.$$

These two equations provide a parametric representation in the (γ_1, γ_2) plane:

$$\sin \nu\gamma_1 = \frac{\nu^2 + 2\omega - 1}{2\nu\omega} \text{ and } \sin \nu\gamma_2 = \frac{\nu^2 - 2\omega + 1}{2\nu(1-\omega)}. \tag{18}$$

The feasibility of solutions requires that

$$-1 \le \frac{\nu^2 + 2\omega - 1}{2\nu\omega} \le 1 \tag{19}$$

and

$$-1 \le \frac{\nu^2 - 2\omega + 1}{2\nu(1-\omega)} \le 1. \tag{20}$$

Consider first condition (19), which is a pair of quadratic inequalities in ν,

$$\nu^2 + 2\nu\omega + 2\omega - 1 \ge 0 \tag{21}$$

and

$$\nu^2 - 2\nu\omega + 2\omega - 1 \le 0 \tag{22}$$

The roots of (21) are -1 and $1-2\omega$, and the roots of (22) are $2\omega-1$ and 1. Condition (20) is also a pair of quadratic inequalities,

$$\nu^2+2\nu(1-\omega)+(1-2\omega)\begin{cases}\geq 0 & \text{if } \omega<1\\ \\ \leq 0 & \text{if } \omega>1\end{cases} \tag{23}$$

and

$$\nu^2-2\nu(1-\omega)+(1-2\omega)\begin{cases}\leq 0 & \text{if } \omega<1\\ \\ \geq 0 & \text{if } \omega>1\end{cases} \tag{24}$$

with -1 and $2\omega-1$ being the roots of (23) and $1-2\omega$ and 1 being the roots of (24). So if $\omega<1$, then the value of ν has to satisfy the following relation:

$$2\omega-1\leq\nu\leq 1.$$

Similarly, if $\omega>1$, then the value of ν has to satisfy relation

$$1\leq\nu\leq 2\omega-1.$$

Since the feasibility domains for $\omega<1$ and $\omega>1$ are different, we discuss these cases separately. As it was explained earlier, we have assumed that $\omega\geq 1/2$. The remaining part of this section is divided into three subsections. First, the non-symmetric case (i.e., $1>\omega>1/2$) is examined in Section 4.1, then the extrapolation case (i.e., $\omega>1$) in Section 4.2 and finally we will turn our attention to the symmetric case (i.e., $\omega=1/2$) in Section 4.3.

4.1 The Case of $\frac{1}{2}<\omega<1$

In this subsection, we assume that $1/2<\omega<1$. Since from (14), we see that the signs of $\cos\nu\gamma_1$ and $\cos\nu\gamma_2$ are different, equations (18) imply that

$$L_1(k,n):\begin{cases}\gamma_1=\dfrac{1}{\nu}\left(\sin^{-1}\left(\dfrac{\nu^2+2\omega-1}{2\nu\omega}\right)+2k\pi\right) & (k\geq 0)\\ \\ \gamma_2=\dfrac{1}{\nu}\left(\pi-\sin^{-1}\left(\dfrac{\nu^2-2\omega+1}{2\nu(1-\omega)}\right)+2n\pi\right) & (n\geq 0)\end{cases} \tag{25}$$

or

$$L_2(k,n):\begin{cases}\gamma_1=\dfrac{1}{\nu}\left(\pi-\sin^{-1}\left(\dfrac{\nu^2+2\omega-1}{2\nu\omega}\right)+2k\pi\right) & (k\geq 0)\\ \\ \gamma_2=\dfrac{1}{\nu}\left(\sin^{-1}\left(\dfrac{\nu^2-2\omega+1}{2\nu(1-\omega)}\right)+2n\pi\right) & (n\geq 0)\end{cases} \tag{26}$$

which gives two sets of parametric curves in the (γ_1,γ_2) plane. The domain of ω is the interval $[2\omega-1,1]$. At the initial point $\nu=2\omega-1$, we have

$$\frac{\nu^2+2\omega-1}{2\nu\omega}=1 \text{ and } \frac{\nu^2-2\omega+1}{2\nu(1-\omega)}=-1$$

and at the end point $\nu = 1$, we have

$$\frac{\nu^2 + 2\omega - 1}{2\nu\omega} = 1 \text{ and } \frac{\nu^2 - 2\omega + 1}{2\nu(1-\omega)} = 1.$$

Therefore the initial and end points of $L_1(k,n)$ are

$$I_1(k,n) = \left(\frac{1}{2\omega - 1}\left(\frac{\pi}{2} + 2k\pi\right),\ \frac{1}{2\omega - 1}\left(\frac{3\pi}{2} + 2n\pi\right)\right)$$

and

$$E_1(k,n) = \left(\frac{\pi}{2} + 2k\pi,\ \frac{\pi}{2} + 2n\pi\right).$$

and similarly, the initial and end points of $L_2(k,n)$ are

$$I_2(k,n) = \left(\frac{1}{2\omega - 1}\left(\frac{\pi}{2} + 2k\pi\right),\ \frac{1}{2\omega - 1}\left(-\frac{\pi}{2} + 2n\pi\right)\right)$$

and

$$E_2(k,n) = \left(\frac{\pi}{2} + 2k\pi,\ \frac{\pi}{2} + 2n\pi\right).$$

Notice that $E_1(k,n) = E_2(k,n)$ and $I_1(k,n) = I_2(k,n+1)$, that is, $L_1(k,n)$ and $L_2(k,n)$ have the same end points and $L_1(k,n)$ and $L_2(k,n+1)$ have the same initial points. Hence the segments

$$(L_2(k,0),\ L_1(k,0), L_2(k,1),\ L_1(k,1), L_2(k,2),\ L_1(k,2), ...)$$

starting at $I_2(k,0)$ and passing through points

$$E_2(k,0) = E_1(k,0),\ I_1(k,0) = I_2(k,1),\ E_2(k,1) = E_1(k,1), ...$$

form a continuous curve.

Figure 2 illustrates the loci $L_1(k,n)$ and $L_2(k,n)$ with the value of ν varying from $2\omega - 1$ to unity for $n = 0, 1, 2$ and $k = 0$. The parameter value $\omega = 0.8$ is selected. The red curves are $L_1(k,n)$ and the blue curves are $L_2(k,n)$. The red and blue curves shift upward when n increases and rightward when k increases. There the initial point $I_2(0,0)$ is infeasible, and $L_2(0,0)$ is feasible only for $\nu \geq \sqrt{2\omega - 1}$. Notice that $I_1(0,n) = I_2(0,n+1)$ at point I_n for $n = 0, 1$ and $E_1(0,n) = E_2(0,n)$ at point E_n for $n = 0, 1, 2$. $\gamma_1^m \simeq 1.493$ is the minimum γ_1-value of the segment $L_1(0,n)$ while $\gamma_1^M \simeq 2.733$ is the maximum γ_1-value of the segment $L_2(0,n)$. It can be checked that $\gamma_1^0 \simeq 2.354$ is the γ_1-value of the intersection of the segment $L_2(0,0)$ with the horizontal axis and is identical with γ_1^* given in Theorem 3. The partition curve stays within the interval $[\gamma_1^m, \gamma_1^M]$ when $k = 0$ but its shape could be different for a different value of ω. It will be shown that the steady state is locally asymptotically stable in the yellow region

of Figure 2.

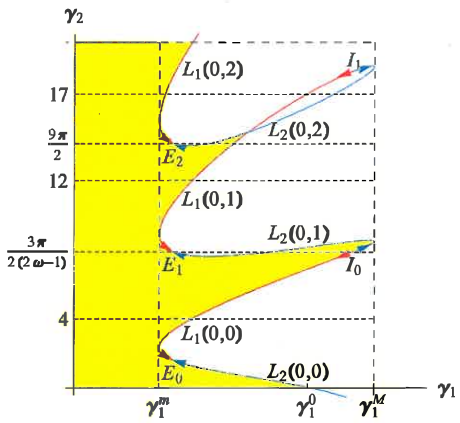

Figure 2. Partition curves with $k = 0$ and $n = 0, 1, 2$

Apparently $\gamma_1^m < \gamma_1^0$ implying that the steady state is locally asymptotically stable for $0 < \gamma_1 < \gamma_1^m$ and $\gamma_2 = 0$ due to Theorem 3. Since the segment $L_i(0, n)$ is in the interval $[\gamma_1^m, \gamma_1^M]$, there are no eigenvalues changing the sign of the real part when γ_2 increases. In other words, the real parts of the eigenvalues are negative for $\gamma_1 < \gamma_1^m$ and any $\gamma_2 > 0$. Hence the steady state is locally asymptotically stable. Such delays of (γ_1, γ_2) do not affect asymptotic behavior of the steady state and thus are harmless. We summarize this result in the following theorem:

Theorem 4 *If $k = 0$ and $0 < \gamma_1 < \gamma_1^m$, then delay γ_2 is harmless, so the steady state is locally asymptotically stable.*

We now move to the case of $\gamma_1 > \gamma_1^m$ and examine the directions of the stability switches by selecting γ_1 as the bifurcation parameter with fixed value of γ_2. So we consider the eigenvalue as a function of the bifurcation parameter, $\bar{\lambda} = \bar{\lambda}(\gamma_1)$. By implicitly differentiating equation (13) with respect to γ_1, we have

$$\frac{d\bar{\lambda}}{d\gamma_1} + \omega e^{-\bar{\lambda}\gamma_1}\left(-\frac{d\bar{\lambda}}{d\gamma_1}\gamma_1 - \bar{\lambda}\right) + (1-\omega)e^{-\bar{\lambda}\gamma_2}\left(-\frac{d\bar{\lambda}}{d\gamma_1}\gamma_2\right) = 0$$

implying that

$$\frac{d\bar{\lambda}}{d\gamma_1} = \frac{\omega\bar{\lambda}e^{-\bar{\lambda}\gamma_1}}{1 - \omega\gamma_1 e^{-\bar{\lambda}\gamma_1} - (1-\omega)\gamma_2 e^{-\bar{\lambda}\gamma_2}}. \tag{27}$$

Since from (13)

$$(1-\omega)e^{-\bar{\lambda}\gamma_2} = -\bar{\lambda} - \omega e^{-\bar{\lambda}\gamma_1},$$

the right-hand side of equation (27) can be rewritten as

$$\frac{d\bar{\lambda}}{d\gamma_1} = \frac{\omega\bar{\lambda}e^{-\bar{\lambda}\gamma_1}}{1+\bar{\lambda}\gamma_2+\omega(\gamma_2-\gamma_1)e^{-\bar{\lambda}\gamma_1}}.$$

If $\bar{\lambda} = i\nu$, then

$$\frac{d\bar{\lambda}}{d\gamma_1} = \frac{i\nu\omega\left(\cos\nu\gamma_1 - i\sin\nu\gamma_1\right)}{1+i\nu\gamma_2+\omega(\gamma_2-\gamma_1)\left(\cos\nu\gamma_1 - i\sin\nu\gamma_1\right)}. \tag{28}$$

Its real part is

$$\mathrm{Re}\left[\frac{d\bar{\lambda}}{d\gamma_1}\right] = \frac{\nu\omega\left[\sin\nu\gamma_1 + \nu\gamma_2\cos\nu\gamma_1\right]}{(1+\omega(\gamma_2-\gamma_1)\cos\nu\gamma_1)^2 + (\nu\gamma_2 - \omega(\gamma_2-\gamma_1)\sin\nu\gamma_1)^2}, \tag{29}$$

As is already shown in Theorem 3, the steady state is asymptotically stable for $\gamma_1 = 0$ and any $\gamma_2 > 0$. Gradually increasing the value of γ_1 with fixed value of γ_2, the horizontal line crosses either $L_1(0,n)$ or $L_2(0,n)$. Consider first the intercept with the segment $L_1(0,n)$. Since both $\sin\nu\gamma_1$ and $\cos\nu\gamma_1$ are positive for $\nu\gamma_1 \in (0,\pi/2)$,

$$\mathrm{Re}\left[\frac{d\bar{\lambda}}{d\gamma_1}\right] > 0.$$

This inequality implies that as γ_1 increases, stability is lost when γ_1 crosses the segment $L_1(0,n)$. In the case of the linear learning process, local instability leads to global instability. However this is not necessary true if the learning process is nonlinear. To confirm global behavior, two bifurcation diagrams generated by the delay logistic equation (8) are illustrated.[3] In particular, we vary γ_1 from γ_1^m to γ_1^M in 0.01 increments, calculate 1000 values for each value of γ_1 and use the last 300 values to get rid of the transients. The local maximum and minimum values of the trajectory are plotted against γ_1 to construct a bifurcation diagram of a^e with respect to γ_1. In Figure 3(A), γ_2 is fixed at 4 and γ_1 increases along the lowest horizontal dotted line of Figure 2. The stable steady state loses stability at $\gamma_1^P \simeq 1.691$, the intersection with the segment $L_1(0,0)$.[4] The bifurcation diagram in Figure 3(A) takes a distorted C-shape and its upper part is thick, indicating that trajectories are quasi-periodic with minor fluctuations in their local maximum values for $\gamma_1 > \gamma_1^P$. It is further seen that the periodic cycle expands as γ_1 becomes larger. In Figure 3(B), γ_2 is changed to 12 and γ_1 increases along the third highest horizontal dotted line of Figure 2. The stability is lost at $\gamma_1^P \simeq 1.80$ where the dotted line crosses the segment $L_1(0,1)$

[3] The linear equation (7) with two delays generates the same simple dynamics as the linear equation (3) with one delay. So no further considerations are given to it.

[4] Using the second equation of (25), we solve equation

$$4 = \frac{1}{\nu}\left(\pi - \sin^{-1}\left(\frac{\nu^2 - 2\omega + 1}{2\nu(1-\omega)}\right)\right)$$

for ν and then substitute the solution into the first equation of (25) to obtain the value of γ_1^P.

from the left.[5] As γ_1 gets larger than γ_1^P, erratic (chaotic) behavior emerges via a period-doubling bifurcation. Further increasing γ_1 suddenly reduces complex dynamics to simple periodic oscillations for γ_1 being close to γ_1^M. Only the values of γ_2 are different between these two diagrams. So a larger γ_2 can be a source of erratic oscillations of $a^e(t)$. These results are numerically confirmed and thus summarized as follows:

Proposition 1 *The steady state loses local stability when increasing γ_1 crosses the segment $L_1(0,n)$ from left for the first time and global behavior of the unstable steady state exhibits simple oscillations if γ_2 is relatively small and complex oscillations if γ_2 is relatively large.*

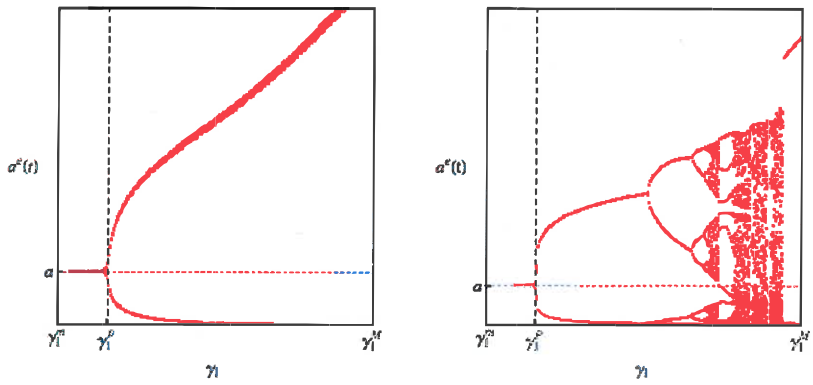

(A) $\gamma_2 = 4$ (B) $\gamma_2 = 12$

Figure 3. Bifurcation diagram I

Assume next that γ_1 crosses a segment $L_2(0,n)$ where $\cos\nu\gamma_1 < 0$ as $\nu\gamma_1 \in (\pi/2,\ \pi)$. It is clear from (29) that

$$\mathrm{Re}\left[\frac{d\bar{\lambda}}{d\gamma_1}\right] = -\frac{\nu^3\omega\cos\nu\gamma_1}{(1+\omega(\gamma_2-\gamma_1)\cos\nu\gamma_1)^2+(\nu\gamma_2-\omega(\gamma_2-\gamma_1)\sin\nu\gamma_1)^2}\frac{\partial\gamma_2}{\partial\nu} \tag{30}$$

where, by implicitly differentiating the second equation in (18) and using (14), we have

$$\frac{\partial\gamma_2}{\partial\nu} = -\frac{1}{\nu^2}\frac{\sin\nu\gamma_1+\nu\gamma_2\cos\nu\gamma_1}{\cos\nu\gamma_1}.$$

Since the first factor with the minus sign of (30) is positive, stability is switched to instability when $\partial\gamma_2/\partial\nu > 0$ and instabiliy might be switched to stability when $\partial\gamma_2/\partial\nu < 0$. Although it is possible to confirm analytically the sign of the

[5] See footnote 4 for detailed arguments to determine γ_1^P.

derivative $\partial\gamma_2/\partial\nu$ on the segment $L_2(0,n)$, we numerically check it.[6] We also examine responses of the nonlinear learning as a function of γ_1 for two different fixed values of γ_2,

$$\gamma_2 = \frac{3\pi}{2(2\omega-1)} \text{ and } \gamma_2 = \frac{9\pi}{2}.$$

We start with $\gamma_2 = 3\pi/(2(2\omega-1)) \simeq 7.85$. Although it is not clear in Figure 2, the segment $L_2(0,1)$ takes a convex-concave shape. So the dotted horizontal line at $3\pi/(2(2\omega-1))$ could have multiple intersects with $L_2(0,1)$. The second equation of (26) determines a value of γ_2. So solving the following equation

$$\frac{3\pi}{2(2\omega-1)} = \frac{1}{\nu}\left(\sin^{-1}\left(\frac{\nu^2-2\omega+1}{2\nu(1-\omega)}\right)+2\pi\right)$$

with $\omega = 0.8$ for ν yields three solutions,

$$\nu_a = 1,\ \nu_b \simeq 0.84, \text{ and } \nu_c = 0.6,$$

each of which is then substituted into the first equation of (26) to obtain three corresponding values of γ_1,

$$\gamma_1^a = \frac{\pi}{2} \simeq 1.57,\ \gamma_1^b \simeq 2.15, \text{ and } \gamma_1^c = \frac{\pi}{2(2\omega-1)} \simeq 2.62.$$

Notice that γ_1^a and γ_1^c are the γ_1-values of the points E_1 and I_0 in Figure 2. Fixing the parameters γ_2 at $3\pi/(2(2\omega-1))$, we perform simulations of equation (8) for different γ_1 values to confirm two dynamic results; one is the appearance and disappearance of a limit cycle for $\gamma_1^a < \gamma_1 < \gamma_1^b$ and the other is initial point dependency of dynamics for $\gamma_1^b < \gamma_1 < \gamma_1^c$. We will discuss these results in detail.

Characterization of bifurcation occurring along the dotted line is given. Start with Figure 4(A). The steady state is locally stable for $\gamma_1^m < \gamma_1 < \gamma_1^a$ and loses stability for $\gamma_1 = \gamma_1^a$ at which $\partial\gamma_2/\partial\nu > 0$ implying that the real part of an eigenvalue is positive for $\gamma_1 > \gamma_1^a$. With further increasing γ_1, it bifurcates to a limit cycle which first expands, then shrinks and finally merges to the steady state to regain stability for $\gamma_1 = \gamma_1^b$. There $\partial\gamma_2/\partial\nu < 0$ implies that the real part of the same eigenvalue becomes negative again for $\gamma_1 > \gamma_1^b$. For $\gamma_1^b < \gamma_1 < \gamma_1^c$, the steady state is locally asymptotically stable as the dotted line is in the yellow region of Figure 2. In order to examine global behavior, we simulate the nonlinear learning process with a constant initial function defined for $t \leq 0$ having slightly different constant values, $\varphi(t) = 0.2$, $\varphi(t) = 0.4$, $\varphi(t) = 0.6$ and $\varphi(t) = 0.8$. Two results are numerically confirmed: the first is that the learning process generates the same dynamics regardless of the different initial functions if $\gamma_1 \leq \gamma_1^b$ or $\gamma_1 > \gamma_1^c$; the second is that for $\gamma_1^b < \gamma_1 < \gamma_1^c$, a trajectory converges to the steady state when $\varphi(t) = 0.8$[7] while it bifurcates to a periodic

[6] See Matsumoto and Szidarovszky (2012d) for analytical examinations of the sign of the derivative.

[7] It is numerically verfied that trajectories converge to the steady state for any initial values close to a (i.e., unity)

cycle by discontinuous jump when any other initial function is selected and further, the jumping value of γ_1 depends on the selection of the initial function. In particular, the green trajectory with $\varphi(t) = 0.2$ jumps to the periodic cycle at the first dotted point in Figure 4(A), the orange trajectory with $\varphi(t) = 0.4$ at the second dotted point, the blue trajectory with $\varphi(t) = 0.6$ at the third dotted point and finally the red trajectory with $\varphi(t) = 0.8$ at the fourth dotted point. Depending on a choice of the initial function, the same delay equation generates different global dynamics.

In Figure 4(B), γ_2 is increased to $9\pi/2 \simeq 14.14$ and the horizontal dotted line at $9\pi/2$ crosses the segment $L_2(0,2)$ twice at the points

$$\gamma_1^a = \frac{\pi}{2} \simeq 1.57 \text{ and } \gamma_1^b \simeq 1.78.$$

Stability is lost at $\gamma_1 = \gamma_1^a$ for which the dotted line crosses $L_2(0,2)$ with $\partial\gamma_2/\partial\nu > 0$ and regained at $\gamma_1 = \gamma_1^b$ for which the dotted line crosses $L_2(0,2)$ with $\partial\gamma_2/\partial\nu < 0$. The dotted line also crosses the segment $L_1(0,1)$ with $\partial\gamma_2/\partial\nu > 0$ at

$$\gamma_1^c \simeq 1.93$$

for which stability is lost again. Taking $\varphi(t) = 0.9$, we simulate the model and obtain the following results. The appearance and disappearance of a limit cycle for $\gamma_1^a < \gamma_1 < \gamma_1^b$ is observed again. Although the initial point dependency is observed in the interval (γ_1^b, γ_1^c) in this case as well, we omit it from Figure 4(B) to avoid the messy bifurcation diagram. Instead, it should be noticed that complex behavior emerges via a period doubling bifurcation for $\gamma_1^c < \gamma_1 < \gamma_1^M$. Comparing these bifurcation diagrams where only the values of γ_2 are different leads to the same conclusion that a larger γ_2 can be a source of erratic oscillations of $a^e(t)$.

Proposition 2 *When the horizontal line of γ_1 crosses the segment of $L_2(0,n)$ for the first time from left, then three different dynamics emerge; (1) the steady state bifurcates to a limit cycle that expands, shrinks and then merges to the steady state for $\gamma_1^a < \gamma_1 < \gamma_1^b$; (2) depending on a choice of the initial functions, it becomes locally asymptotically stable or bifurcates to a periodic oscillation for $\gamma_1^b < \gamma_1 < \gamma_1^c$; (3) it proceeds to a periodic oscillation or chaos via a period-doubling cascade for $\gamma_1^c < \gamma_1 < \gamma_1^M$ according to whether γ_2 is small or large.*

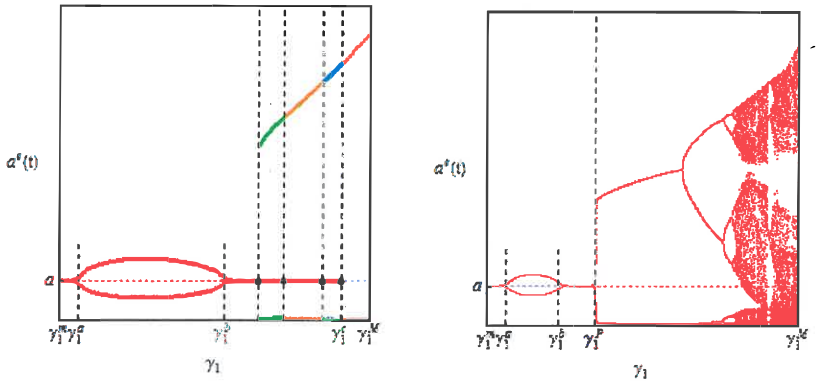

(A) $\gamma_2 = \frac{3\pi}{2(2\omega-1)}$ (B) $\gamma_2 = \frac{9\pi}{2}$

Figure 4. Bifurcation diagram II

In the next simulation, γ_2 is increased to 17 and then kept fixed. γ_1 is increased along the highest horizontal dotted line of Figure 2. As can be seen, the horizontal line has three intercepts. At the first one with $L_1(0,2)$ the steady state becomes unstable. At the second one with $L_1(0,1)$ the real part of one more eigenvalue becomes positive. At the third intercept with $L_2(0,2)$ the real part of only one of the two eigenvalues changes back to negative. Therefore stability cannot be regained at this point, so no stability switch occurs. According to Figure 5, the steady state is replaced with a periodic oscillation just after it becomes unstable and there is a very short period-doubling cascade to chaos. As we can see further, interesting dynamics begins; complex dynamics suddenly disappears and a periodic oscillation appears and undergoes a period-doubling

bifurcation cascade to chaos again.

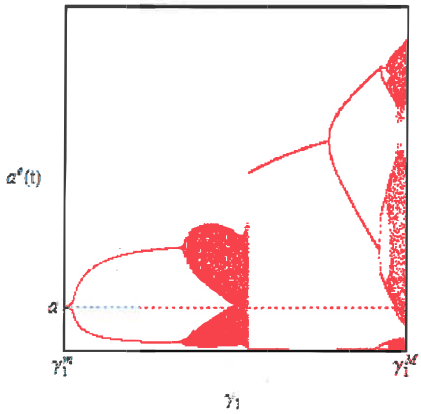

Figure 5. Bifurcation diagram III

Let us summarize the main point that has been made so far.

Proposition 3 *(1) Given $k = 0$, the boundary of the stable region consists of the envelop of the segments $L_1(0,n)$ and $L_2(0,n)$ for $n \geq 0$; (2) depending values of (γ_1, γ_2), the nonlinear learning process can generate a wide spectrum of dynamics ranging from simple periodic oscillations to complex aperiodic oscillations when the steady state loses local stability.*

We can also show that at stability switches only one eigenvalue changes the sign of its real part, that is, the pure complex eigenvalues are single. Assume not, then $\bar{\lambda} = i\nu$ solves both equations

$$\bar{\lambda} + \omega e^{-\bar{\lambda}\gamma_1} + (1-\omega)e^{-\bar{\lambda}\gamma_2} = 0 \tag{31}$$

and

$$1 - \omega\gamma_1 e^{-\bar{\lambda}\gamma_1} - (1-\omega)\gamma_2 e^{-\bar{\lambda}\gamma_2} = 0 \tag{32}$$

from which we have

$$e^{-\bar{\lambda}\gamma_1} = \frac{1+\bar{\lambda}\gamma_2}{(\gamma_1-\gamma_2)\omega} \text{ and } e^{-\bar{\lambda}\gamma_2} = \frac{-1-\bar{\lambda}\gamma_1}{(\gamma_1-\gamma_2)(1-\omega)}. \tag{33}$$

If $\bar{\lambda} = i\nu$, then by comparing the real and imaginary parts, we conclude that

$$\sin\nu\gamma_1 + \nu\gamma_2\cos\nu\gamma_1 = \sin\nu\gamma_2 + \nu\gamma_1\cos\nu\gamma_2 = 0$$

or

$$\tan\nu\gamma_1 + \nu\gamma_2 = \tan\nu\gamma_2 + \nu\gamma_1 = 0. \tag{34}$$

Let $L_i(k,n)$ denote the segment containing (γ_1,γ_2), then this point is a common extremum of $L_i(k,n)$ with respect to γ_1 and γ_2, which is impossible, since $L_i(k,n)$ is a differentiable curve.

Until this point, we examined the curves $L_1(k,n)$ and $L_2(k,n)$ for $k=0$. If $k\geq 1$, then these curves are shifted to the right and slightly modified resulting in similar patterns. If we fix the value of γ_2 and gradually increase the value of γ_1 from zero, then it is unknown theoretically how the stability region, if any, looks like behind the $L_1(0,n)$ and $L_2(0,n)$ curves. By performing repeated simulations no stability region was found here.

Consider now a point (γ_1^*,γ_2^*) with positive coordinates, and consider the horizontal line $\gamma_2=\gamma_2^*$ and its segment for $0\leq\gamma_1\leq\gamma_1^*$. There are finitely many intercepts of this horizontal segment with the set

$$L=\cup_{n=0}^{\infty}\cup_{k=0}^{\infty}\left\{L_1(k,n)\cup L_2(k,n)\right\}.$$

Let $s(\gamma_1^*,\gamma_2^*)$ denote the number of intercepts where stability is lost and $g(\gamma_1^*,\gamma_1^*)$ the number of intercepts where stability can be regained. With (γ_1^*,γ_2^*) the system is asymptotically stable if $g(\gamma_1^*,\gamma_2^*)\geq s(\gamma_1^*,\gamma_2^*)$ and unstable otherwise. The stability region is illustrated as the yellow domain in Figure 2.

4.2 The Case of $\omega>1$

From (14) we see that $\cos(\nu\gamma_1)$ and $\cos(\nu\gamma_2)$ must have the same sign, so in this case we have also two types of segments,

$$L_1(k,n):\begin{cases}\gamma_1'=\dfrac{1}{\nu}\left(\sin^{-1}\left(\dfrac{\nu^2+2\omega-1}{2\nu\omega}\right)+2k\pi\right)\ (k\geq 0)\\[2ex]\gamma_2'=\dfrac{1}{\nu}\left(\sin^{-1}\left(\dfrac{\nu^2-2\omega+1}{2\nu(1-\omega)}\right)+2n\pi\right)\ (n\geq 0)\end{cases}\tag{35}$$

and

$$L_2(k,n):\begin{cases}\gamma_1'=\dfrac{1}{\nu}\left(\pi-\sin^{-1}\left(\dfrac{\nu^2+2\omega-1}{2\nu\omega}\right)+2k\pi\right)\ (k\geq 0)\\[2ex]\gamma_2'=\dfrac{1}{\nu}\left(\pi-\sin^{-1}\left(\dfrac{\nu^2-2\omega+1}{2\nu(1-\omega)}\right)+2n\pi\right)\ (n\geq 0)\end{cases}\tag{36}$$

where $1\leq\nu\leq 2\omega-1$. As in the previous case, at $\nu=1$,

$$\frac{\nu^2+2\omega-1}{2\nu\omega}=1 \text{ and } \frac{\nu^2-2\omega+1}{2\nu(1-\omega)}=1$$

and at $\nu=2\omega-1$,

$$\frac{\nu^2+2\omega-1}{2\nu\omega}=1 \text{ and } \frac{\nu^2-2\omega+1}{2\nu(1-\omega)}=-1.$$

Therefore the initial and end points of $L_1(k,n)$ are

$$I_1(k,n) = \left(\frac{\pi}{2} + 2k\pi, \frac{\pi}{2} + 2n\pi\right)$$

and

$$E_1(k,n) = \left(\frac{1}{2\omega - 1}\left(\frac{\pi}{2} + 2k\pi\right), \frac{1}{2\omega - 1}\left(-\frac{\pi}{2} + 2n\pi\right)\right)$$

and those of $L_2(k,n)$ are

$$I_2(k,n) = \left(\frac{\pi}{2} + 2k\pi, \frac{\pi}{2} + 2n\pi\right)$$

and

$$E_2(k,n) = \left(\frac{1}{2\omega - 1}\left(\frac{\pi}{2} + 2k\pi\right), \frac{1}{2\omega - 1}\left(\frac{3\pi}{2} + 2n\pi\right)\right).$$

Figure 6 shows the loci $L_1(k,n)$ and $L_2(k,n)$ with the value of ν varying from unity to $2\omega - 1$. The parameter value $\omega = 1.2$ is selected. The red curves are the $L_1(0,n)$ segments and the blue curves are the $L_2(0,n)$ loci. If $n = 0$, then $E_1(k,n)$ is infeasible and $L_1(k,0)$ is feasible only for $\nu \leq \sqrt{2\omega - 1}$. In this case $I_1(k,n) = I_2(k,n)$ and $E_2(k,n) = E_1(k,n+1)$, so $L_1(k,n)$ and $L_2(k,n)$ have the same initial point and $E_1(k,n+1)$ and $E_2(k,n)$ have the same end point. Hence segments

$$(L_1(k,0),\ L_2(k,0),\ L_1(k,1),\ L_2(k,1),\ L_1(k,2),\ L_2(k,2), ...)$$

starting at $E_1(k,0)$ and passing through points

$$I_1(k,0) = I_2(k,0),\ E_2(k,0) = E_1(k,1),\ I_1(k,1) = I_2(k,1),\ E_2(k,1) = E_1(k,2), ...$$

form a continuous curve.

If $\gamma_1 = 0$, then the steady state is asymptotically stable for any $\gamma_2 \geq 0$ according to Theorem 2. If $\gamma_2 = 0$, then the steady state is locally asymptotically stable if $0 < \gamma_1 < \gamma_1^*$ and locally unstable if $\gamma_1 > \gamma_1^*$ according to Theorem 3. We now proceed to the general case of $\gamma_1 > 0$ and $\gamma_2 > 0$. The stability switches with fixed $\gamma_2 > 0$ and increasing values of γ_1 can be discussed similarly to the case of $\omega < 1$, so the details are not given here. Instead of repeating that discussion, we fix the value of $\gamma_1 \in (\gamma_1^m, \gamma_1^M)$, then the vertical line with gradually increasing values of γ_2 crosses $L_1(0,n)$ and $L_2(0,n)$ infinitely many times. We numerically confirm that stability switch could occur at some of those intersections. Consider stability switches first along the vertical dotted line at $\gamma_1^a = 1.2$ and then along the vertical dotted line at $\gamma_1^b = 1.5$ as shown in

Figure 6.

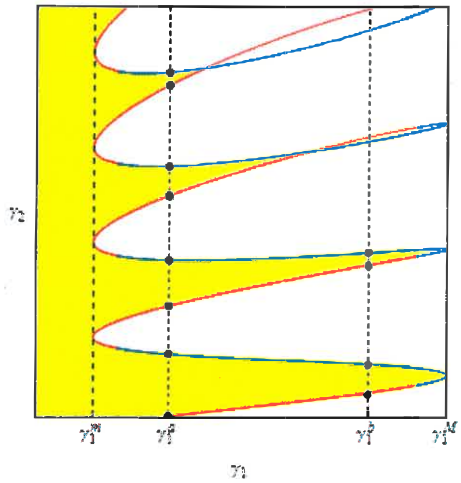

Figure 6. The partition curves with $\omega > 1$

The first numerical result is illustrated in Figure 7(A) where the steady state repeats stability-loss and stability-gain four times and finally becomes unstable. More precisely, stability is lost at the intercepts with $L_2(0,n)$ for $n = 0,1,2,3$ while it is regained at the intercepts with $L_1(0,n)$ for $n = 0,1,2,3$. The system generates only periodic oscillations. The second numerical result is illustrated in Figure 7(B). It can be seen that the system gives rise to periodic oscillations as well for a length of delay approximately less than 10 and to more complex oscillations for a larger value of the delay.

The special case of $\omega = 1$ is identical to the case of a single delay, which was already discussed.

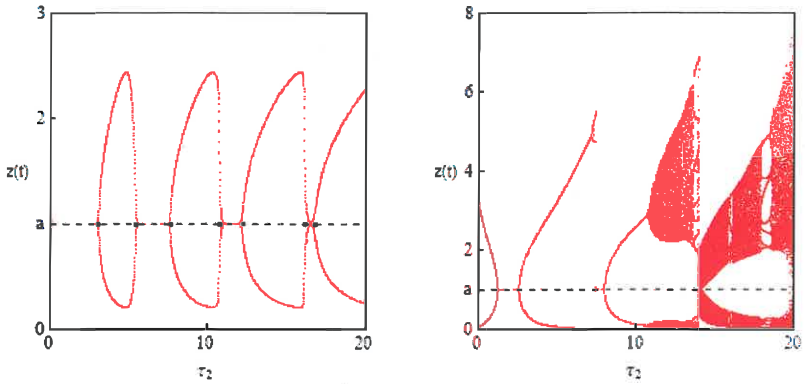

(A) $\gamma_1 = \gamma_1^a$ (B) $\gamma_1 = \gamma_1^b$

Figure 7. Bifurcation diagrams with different values of γ_1

4.3 The Symmetric Case of $\omega = \frac{1}{2}$

If $\omega = 1/2$, then equations (14) and (15) become

$$\cos(\nu\gamma_1) + \cos(\nu\gamma_2) = 0$$

and

$$\nu - \frac{1}{2}\left(\sin(\nu\gamma_1) + \sin(\nu\gamma_2)\right) = 0$$

and the segments $L_1(k,n)$ and $L_2(k,n)$ are simplified as follows:

$$L_1(k,n): \begin{cases} \gamma_1 = \dfrac{1}{\nu}\left(\sin^{-1}(\nu) + 2k\pi\right) & (k \geq 0) \\ \gamma_2 = \dfrac{1}{\nu}\left(\pi - \sin^{-1}(\nu) + 2n\pi\right) & (n \geq 0) \end{cases} \tag{37}$$

and

$$L_1(k,n): \begin{cases} \gamma_1 = \dfrac{1}{\nu}\left(\pi - \sin^{-1}(\nu) + 2k\pi\right) & (k \geq 0) \\ \gamma_2 = \dfrac{1}{\nu}\left(\sin^{-1}(\nu) + 2n\pi\right) & (n \geq 0). \end{cases} \tag{38}$$

Clearly ν has to be in the unit interval in order to have feasible solutions. The segments $L_1(k,n)$ and $L_2(k,n)$ for small values of k and n are illustrated as the red and the blue curves in Figure 8. When $k = n = 0$, these segments construct a hyperbolic curve passing through the point $(\pi/2, \pi/2)$ which is the common point of $L_1(0,0)$ and $L_2(0,0)$. It divides the first quadrant of the (γ_1, γ_2) plane

into two subregions: in the yellow region under the curve, the steady state is locally asymptotically stable and in the white region above, it is locally unstable. Note that the curve is symmetric with respect to the diagonal and asymptotic to the line $\gamma_i = 1$ for $i = 1, 2$. This implies that any delay $\gamma_i > 0$ is harmless if $\gamma_j \leq 1$ for $i, j = 1, 2$ and $i \neq j$.

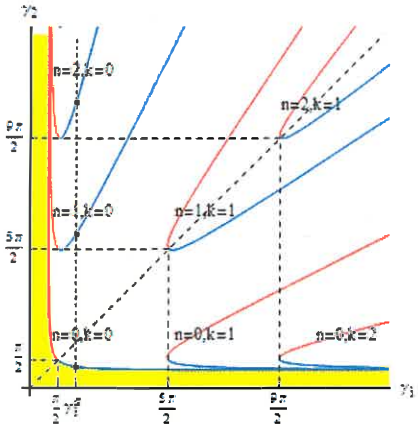

Figure 8. Stability switch curves with $\omega = 0.5$

Two numerical simulations are done with two different values of γ_1. In the first simulation depicted in Figure 9(A), we increase the value of γ_2 from zero to 20 along the vertical dotted line at $\gamma_1 = \pi/2$. The steady state loses stability at $\gamma_2 = \pi/2$ and bifurcates to cyclic oscillations with finite number of periodicity as γ_2 becomes larger. As far as the simulations are concerned, only periodic cycles can be born. In the second simulation shown in Figure 9(B), we change the value of γ_1 to $(\pi/2) + 1$. A limit cycle emerges after stability is lost at $\gamma_2 = \gamma_2^c$ when the increasing value of γ_2 crosses the hyperbolic curve, then exhibits aperiodic

oscillations for γ_2 being about 14 and returns to periodic oscillations afterwards.

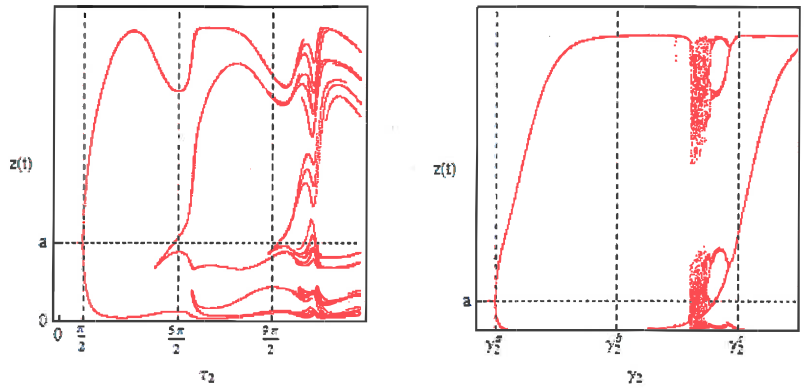

(A) $\gamma_1 = \frac{\pi}{2}$ (B) $\gamma_1 = \frac{\pi}{2} + 1$

Figure 9. Bifurcation diagrams with $\omega = \frac{1}{2}$

5 Conclusion

An adaptive learning process is introduced when the monopoly knows its cost function, the marginal price and uncertain about the maximum price. It is able to update repeatedly its belief of the maximum price by comparing the actual and predicted market prices. It is assumed that the firm's prediction is either the most current delayed price information or it is obtained by interpolation or by extrapolation based on two delayed data. The asymptotical stability of the resulted dynamic learning process is examined. If it is asymptotically stable, then the beliefs of the firm about the maximum price converge to the true value, so successful learning is possible. Stability conditions are derived, the stability regions are determined and illustrated. The global behavior of the trajectory is examined by using simulation.

The dynamic models (5) and (7) are linear, when local asymptotical stability implies global asymptotical stability. However (6) and (8) are nonlinear, where only local asymptotic stability can be guaranteed under the derived conditions. The learning processes (3) and (4) can be generalized as

$$\dot{a}^e(t) = g(a - a^e(t))$$

where function g is sign preserving, that is, for all $\delta \neq 0$,

$$\delta g(\delta) > 0.$$

In our future research, different types of such nonlinear learning schemes will be introduced in our model and we will investigate the asymptotical behavior of the resulted dynamics. Uncertainty and learning of other model parameters will be additional subjects of our study.

References

[1] Bellman, R. and Cooke, K. (1956), *Differential-Difference Equations*, Academic Press, New York.

[2] Burger, E. (1956), On the Stability of Certain Economic Systems, *Econometrica*, 24, 488-493.

[3] Cooke, K. and Grossman, Z. (1992) Discrete Delay Distributed Delay and Stability Switches, *Journal of Mathematical Analysis and Applications*, 86, 592-627.

[4] Cushing, J (1977), *Integro-Difference Equations and Delay Models in Population Dynamics,* Springer-Verlag, Berlin/Heidelberg/New York.

[5] Hayes, N. D. (1950), Roots of the Transcendental Equation Associated with a Certain Difference-Differential Equation, *Journal of the London Mathematical Society*, 25, 226-232.

[6] Invernizzi, S. and Medio, A. (1991), On Lags and Chaos in Economic Dynamic Models, *Journal of Mathematical Economics*, 20, 521-550.

[7] Matsumoto, A. and Szidarovszky, F. (2013), Discrete-Time Delay Dynamics of Boundedly Rational Monopoly, forthcoming in *Decisions in Economics and Finance.*

[8] Matsumoto, A. and Szidarovszky, F. (2012a), Dynamic Monopoly with Multiple Continuously Distributed Time Delays, *IERCU* DP #184 (http://www2.tamacc.chuo-u.ac.jp/keizaiken/discuss.htm), Chuo University.

[9] Matsumoto, A. and Szidarovszky, F. (2012b), Bounded Rational Monopoly with Single Continuously Distributed Time Delay, *IERCU* DP #180 (http://www2.tamacc.chuo-u.ac.jp/keizaiken/discuss.htm), Chuo University.

[10] Matsumoto, A. and Szidarovszky, F. (2012c), An Elementary Study of a Class of Dynamic Systems with Single Time Delay, forthcoming in *CUBO: A Mathematical Journal.*

[11] Matsumoto, A. and Szidarovszky, F. (2012d), Nonlinear Delay Monopoly with Bounded Rationality. *Chaos, Solitons and Fractals*, 45, 507-519.

[12] Naimzada, A. (2012), A Delay Economic Model with Flexible Time Lag, forthcoming in *Chaos, Solitons and Fractals.*

[13] Naimzada, A. and Ricchiuti, G. (2008), Complex Dynamics in a Monopoly with a Rule of Thumb, *Applied Mathematics and Computation*, 203, 921-925.

[14] Puu, T. (1995), The Chaotic Monopolist, *Chaos, Solitons and Fractals*, 5, 35-44.